Thermochimica Acta, 28 (1979) 287–305

INFLUENCE OF THE PREPARATION HISTORY OF α-Fe_2O_3 ON ITS REACTIVITY FOR HYDROGEN REDUCTION

M. SHIMOKAWABE, R. FURUICHI AND T. ISHII
Department of Applied Chemistry, Faculty of Engineering, Hokkaido University, Sapporo 060 (Japan)
(Received 20th February 1978)

ABSTRACT

TG experiments on the hydrogen reduction of α-Fe_2O_3 were carried out to elucidate the influence of the preparation history of the oxide on its reactivity. α-Fe_2O_3 samples were prepared by the thermal decomposition of seven iron salts in a stream of oxygen, air or nitrogen at temperatures of 500–1200°C for 1 h. Thirteen metal ions such as Cu^{2+}, Ni^{2+}, etc. were used as doping agents. The reactivity of the oxide was indicated by the initial reduction temperature (T_i). α-Fe_2O_3 prepared at lower temperatures showed lower T_i values and the reduction proceeded stepwise ($Fe_2O_3 \rightarrow Fe_3O_4 \rightarrow Fe$). T_i values increased with the rise in the preparation temperature of the oxide. The oxides prepared at higher temperatures showed that two reduction steps ($Fe_2O_3 \rightarrow Fe_3O_4$, $Fe_3O_4 \rightarrow Fe$) proceed simultaneously. The preparation in oxygen gave higher T_i than that in air or nitrogen. The doping by metal ions, except Ti^{4+}, lowered the T_i of α-Fe_2O_3. The Cu^{2+} ion showed the lowest T_i, while Ti^{4+} showed the highest T_i and the inhibition effect.

The reduction process was expressed by two equations; Avrami–Erofeev's equation for α-$Fe_2O_3 \rightarrow Fe_3O_4$ and Mampel's equation for $Fe_3O_4 \rightarrow Fe$.

INTRODUCTION

In previous papers[1–3], the catalytic thermal decomposition of solid $KClO_4$ by α-Fe_2O_3 was investigated in order to elucidate the influence of the preparation methods of the oxide on its reactivity. An initial decomposition temperature, easily detected by DTA and/or TG, was used as a reasonable parameter of the reactivity of the oxide. The present paper is concerned with a systematic investigation of the reduction by hydrogen of α-Fe_2O_3 with different preparation histories.

The reduction of iron oxides has been investigated very extensively from scientific and industrial standpoints[4–13]. The different mechanisms are represented for the various types of specimens (powder, pellet and ore) and experimental conditions (temperature, pressure, isothermal, non-isothermal, etc.). The common features being known at present are (1) the reduction of α-Fe_2O_3 proceeds stepwise, (2) at temperatures above 570°C, α-Fe_2O_3 is reduced to Fe metal via Fe_3O_4 and FeO and

(3) below 570 °C, it is reduced via Fe_3O_4 only owing to the instability of FeO. Colombo et al.[4] have reported two reduction processes for different α-Fe_2O_3. They have also shown that the kinetic behavior of the reduction is closely related to the defective structure of the oxide.

In the present work, α-Fe_2O_3 powders with different preparation histories were prepared by calcination of seven iron salts in a stream of oxygen, air or nitrogen, in the temperature range 500–1200 °C, and thirteen metal ions were used for doping. In order to compare the reactivity of α-Fe_2O_3, the initial reduction temperature (T_i) was measured by TG. Isothermal kinetic experiments, X-ray analysis and SEM observation were also carried out to give a clue to the process of the reduction of the oxides.

TABLE 1

METHOD OF PREPARATION OF α-Fe_2O_3

Sample	*Starting material*	*Atmosphere (100ml min^{-1})*	*Temperature (°C)*	*Doping material (M/Fe = 1 mole %)*
α-$Fe_2O_3(S_1)$	$FeSO_4 \cdot 7H_2O$	Air	700–1200	
α-$Fe_2O_3(S_2)$	$Fe_2(SO_4)_3 \cdot xH_2O$	Air	700–1200	
α-$Fe_2O_3(N)$	$Fe(NO_3)_3 \cdot 9H_2O$	Air	500–1200	
α-$Fe_2O_3(C)$	$FeCl_3 \cdot 6H_2O$	Air	500–1200	
α-$Fe_2O_3(A)$	$Fe(OH)(CH_3COO)_2$	Oxygen, air	500–1200	
α-$Fe_2O_3(O)$	$FeC_2O_4 \cdot 2H_2O$	Oxygen, air	500–1200	
α-$Fe_2O_3(H)$	$Fe(OH)_3$	Oxygen, air, nitrogen	500–1200	
α-$Fe_2O_3(S_1D)$	$FeSO_4 \cdot 7H_2O$	Air	700	$LiOH \cdot H_2O$ $Mg(OH)_2$ $Al(OH)_3$ SiO_2(amorphous) $CuSO_4 \cdot 5H_2O$ $NiSO_4 \cdot 6H_2O$ $MnSO_4 \cdot 4$–$5H_2O$ $CoSO_4 \cdot 7H_2O$ $Cr_2(SO_4)_3 \cdot 4H_2O$
α-$Fe_2O_3(OD)$	$FeC_2O_4 \cdot 2H_2O$	Air	500–900	$LiCO_3$ TiO_2(anatase) $CuC_2O_4 \cdot 1/2H_2O$ $MgC_2O_4 \cdot 2H_2O$ $NiC_2O_4 \cdot 2H_2O$ $Ce_2(C_2O_4)_3 \cdot 9H_2O$ $La_2(C_2O_4)_3 \cdot 9H_2O$
α-$Fe_2O_3(MD)$	Fe_3O_4*	Air	600	Li^+ Cu^{2+} B^{3+} Ti^{3+}

* Prepared by precipitation from the equimolar aqueous solution of $FeSO_4$ and $Fe_2(SO_4)_3$ containing various metal ions.

EXPERIMENTAL

Materials

Ten α-Fe_2O_3 samples and their preparation methods are shown in Table 1. Seven iron salts, shown in column 2, were used as the starting materials. Two sulfates were dehydrated in air at 200 °C for 0.5 h and subsequently decomposed to α-$Fe_2O_3(S_1)$ and (S_2) in a stream of air (100 ml min^{-1}) at temperatures of 700–1200 °C for 1 h. These oxides were washed with hot water to remove residual sulfate ions until no $BaSO_4$ precipitate was observed in the filtrates. Five other iron salts were decomposed in a stream of air, oxygen or nitrogen (100 ml min^{-1}) at temperatures of 500–1200 °C for 1 h. The last three samples, α-$Fe_2O_3(S_1D)$, (OD) and (MD) in Table 1 were prepared in order to test the influence of doping by metal ions on the reactivity of the oxide. Nine α-$Fe_2O_3(S_1D)$ samples doped with different metal ion were obtained from the mixtures of $FeSO_4 \cdot 7H_2O$ and doping material ($LiOH \cdot H_2O$, $Mg(OH)_2$, $Al(OH)_3$, SiO_2(amorphous), $CuSO_4 \cdot 5H_2O$, $NiSO_4 \cdot 6H_2O$, $MnSO_4 \cdot 4$–$5H_2O$, $CoSO_4 \cdot 7H_2O$, or $Cr_2(SO_4)_3 \cdot 4H_2O$, M/Fe = 1 mole%). The mixtures were calcined in a stream of air (100 ml min^{-1}) at 700 °C for 1 h. Seven α-Fe_2O_3(OD) samples were prepared from the mixtures of $FeC_2O_4 \cdot 2H_2O$ and doping material [$LiCO_3$, TiO_2(anatase), $CuC_2O_4 \cdot 1/2H_2O$, $MgC_2O_4 \cdot 2H_2O$, $NiC_2O_4 \cdot 2H_2O$, $Ce_2(C_2O_4)_3 \cdot 9H_2O$, or $La_2(C_2O_4)_3 \cdot 9H_2O$, M/Fe = 1 mole%]. The mixtures were calcined in a stream of air (100 ml min^{-1}) at temperatures of 500–900 °C for 1 h. The mixing of iron salt with doping material was carried out in an agate mortar for 1.5 h. Four α-Fe_2O_3(MD) samples were obtained by the oxidation of Fe_3O_4 samples in a stream of air (100 ml min^{-1}) at 600 °C for 1 h. Samples of Fe_3O_4 containing metal ions were prepared from equimolar solution of $FeSO_4$ and $Fe_2(SO_4)_3$ containing $LiNO_3$, $Cu(NO_3)_2$, $Na_2B_4O_7 \cdot 10H_2O$, or $Ti_2(SO_4)_3 \cdot 8H_2O$ (M/Fe = 1 mole%) by use of 6 M NaOH. All oxides prepared were confirmed to be α-Fe_2O_3 by X-ray diffraction patterns. The iron salts and other materials used were GR reagents from Kanto Chemical Co. In what follows, the preparation temperature of the oxide will be indicated by, for example, α-Fe_2O_3 (A-500) in which 500 correspond to the temperature (°C).

TG and DTG

TG and DTG apparatus employed were a Cahn electrobalance Model RG with a quartz hung-down tube (d = 35 mm) and a Cahn time derivative computer Mark II. A 30 mg α-Fe_2O_3 was placed in a cylindrical quartz dish (10 × 10 mm). The measurements were carried out at a heating rate of 4.5 °C min^{-1} and a chromel–alumel thermocouple was used for the temperature measurements. Before the experiment, the sample was evacuated at 10^{-3} mm Hg, and then the reduction was carried out in the mixture of H_2(50 mm Hg) and N_2(100 mm Hg). A preliminary experiment showed that the gas pressure of 150 mm Hg gave no buoyance effect up to 900 °C. In isothermal experiments, after the sample was heated to a fixed temperature in 150 mm

Hg nitrogen, the apparatus was evacuated, and subsequently the reduction gas mixture was introduced to start the reduction.

The initial reduction temperature (T_i)

The value of initial reduction temperature (T_i) was determined by measuring the onset temperature of weight decrease on the TG curve. The accuracy of T_i was $\pm$ 5°C.

X-Ray diffraction and scanning electron microscopy (SEM)

The X-ray diffractometer used was of the Geigerflex 2001 type (Rigaku Denki Co.), and operated under the following conditions; Co target, Fe filter, 35 kV and 10 mA. The SEM apparatus used was of the MSM-4 type (Hitachi–Akashi Co.). The SEM sample was coated with gold film (ca. 300 Å) by using Ion Coater IB-3 (Eiko Eng. Co.).

Specific surface area and crystallite size

The specific surface area of α-Fe_2O_3 was estimated by BET from the amount of N_2 adsorbed at -195°C. The crystallite size was calculated from the line width of the X-ray diffraction line by Scherrer's method.

RESULTS

Influence of preparation temperature and starting materials

Figure 1 shows (A) TG and (B) DTG curves of the hydrogen reduction of α-Fe_2O_3(A) samples prepared in air, and (C) X-ray diffraction patterns of partially reduced samples. Four TG curves (a)–(d) are the results for α-Fe_2O_3(A) prepared at 500, 700, 900 and 1200°C, respectively. These samples can be divided into two groups, (I) and (II). The first group (I) consists of samples prepared at lower temperatures, 500 and 700°C, which show the plateau at 11.1% weight decrease. The value of 11.1% corresponds to the formation of Fe_3O_4. The formation of only Fe_3O_4 at 11.1% is confirmed by X-ray diffraction of 11.1%-reduced oxide as shown in Fig. 1(C) (i). It is thought, therefore, that the reduction of α-Fe_2O_3 prepared at lower temperatures proceeds stepwise through reactions (1) and (2).

$$3\,Fe_2O_3 + H_2 \rightarrow 2\,Fe_3O_4 + H_2O \quad (1)$$

$$Fe_3O_4 + 4\,H_2 \rightarrow 3\,Fe + 4\,H_2O \quad (2)$$

The DTG curve of α-Fe_2O_3 (A-500) in Fig. 1(B) (a) shows two peaks at 350°C and 550°C corresponding to reactions (1) and (2), respectively. On the other hand, the oxides of the second group (II) are those prepared at 900 and 1200°C, which do not show the plateau at 11.1%. The X-ray diffraction pattern of 11.1%-reduced α-Fe_2O_3 (A-1200), Fig. 1(C) (ii), shows that this partially reduced sample was a mixture of α-Fe_2O_3, Fe_3O_4 and metallic Fe, and DTG curve of α-Fe_2O_3 (A-1200),

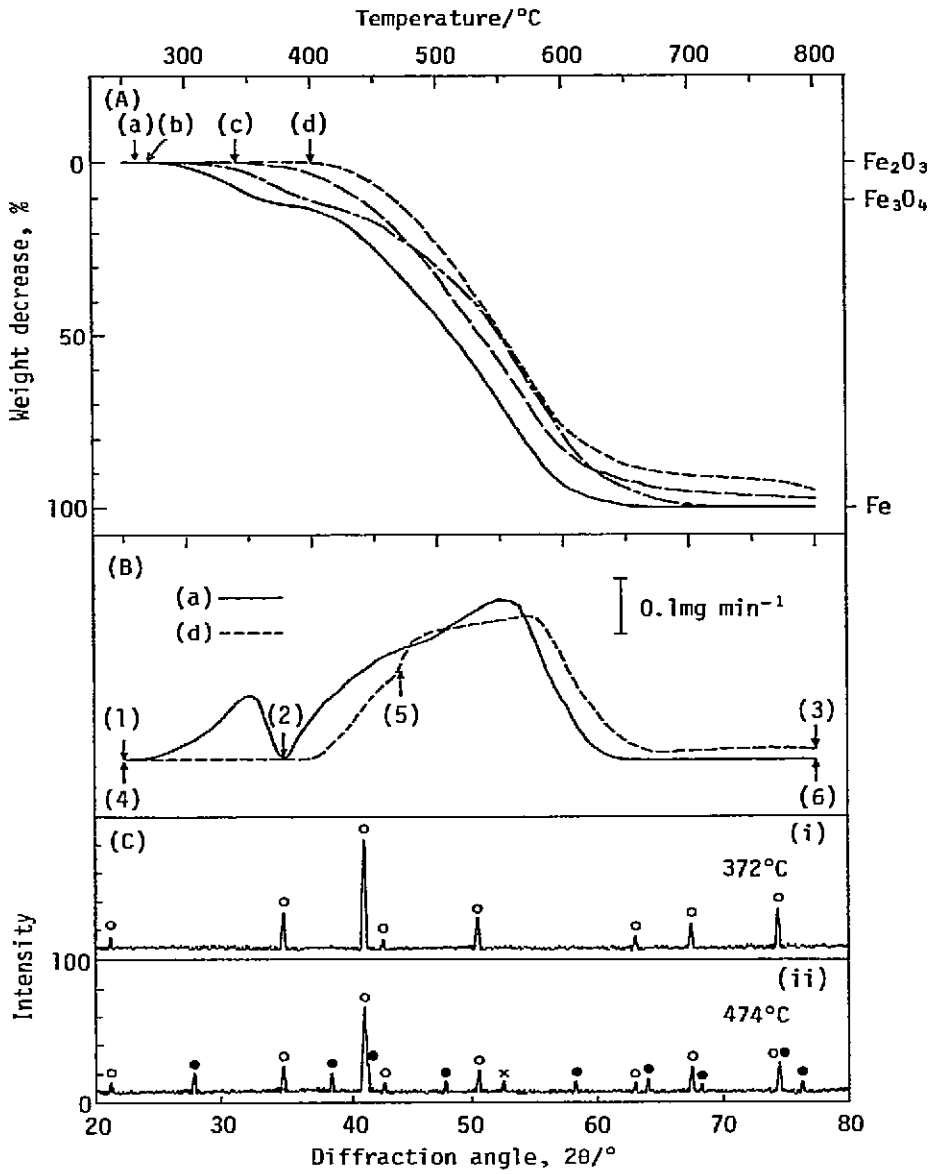

Fig. 1. (A) TG and (B) DTG curves of the hydrogen reduction of α-Fe_2O_3(A), and (C) X-ray diffraction patterns of partially reduced samples up to 372 °C and 474 °C. (A) and (B), (a) —, α-Fe_2O_3 (A-500); (b) —·—, α-Fe_2O_3(A-700); (c) ——, α-Fe_2O_3(A-900); (d) ----, α-Fe_2O_3(A-1200). ↓ = Initial reduction temperature (T_i). (C), (i) α-Fe_2O_3(A-500) reduced up to 372 °C; (ii) α Fe_2O_3(A 1200) reduced up to 474 °C. ●, α Fe_2O_3; ○, Fe_3O_4; ×, α Fe.

Fig. 1(B) (d), shows a broad peak at 500–600 °C. Therefore, in the reduction for the second group, reactions (1) and (2) proceed simultaneously. The arrows on the TG curves indicate the initial reduction temperature (T_i) of α-Fe_2O_3(A). The T_i value increases from 260 to 400 °C with the rise in the preparation temperature. It is observed for all oxides that the reduction rate becomes slower above 600 °C, and the oxides prepared at higher temperature, such as α-Fe_2O_3(A-900) and α-Fe_2O_3(A-1200), are not reduced completely even at 800 °C. The presence of FeO, which is known to be

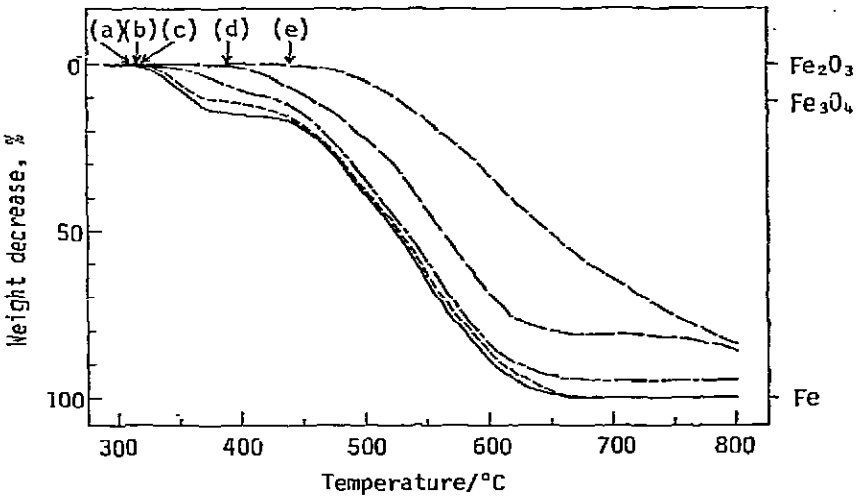

Fig. 2. TG curves of the hydrogen reduction of α-Fe_2O_3(S_1). (a) —, α-Fe_2O_3(S_1-700); (b) -------, α-Fe_2O_3(S_1-800); (c) —·—, α-Fe_2O_3(S_1-900); (d) ——, α-Fe_2O_3(S_1-1000); (e) – – –, α-Fe_2O_3(S_1-1200). ↓ = Initial reduction temperature (T_i).

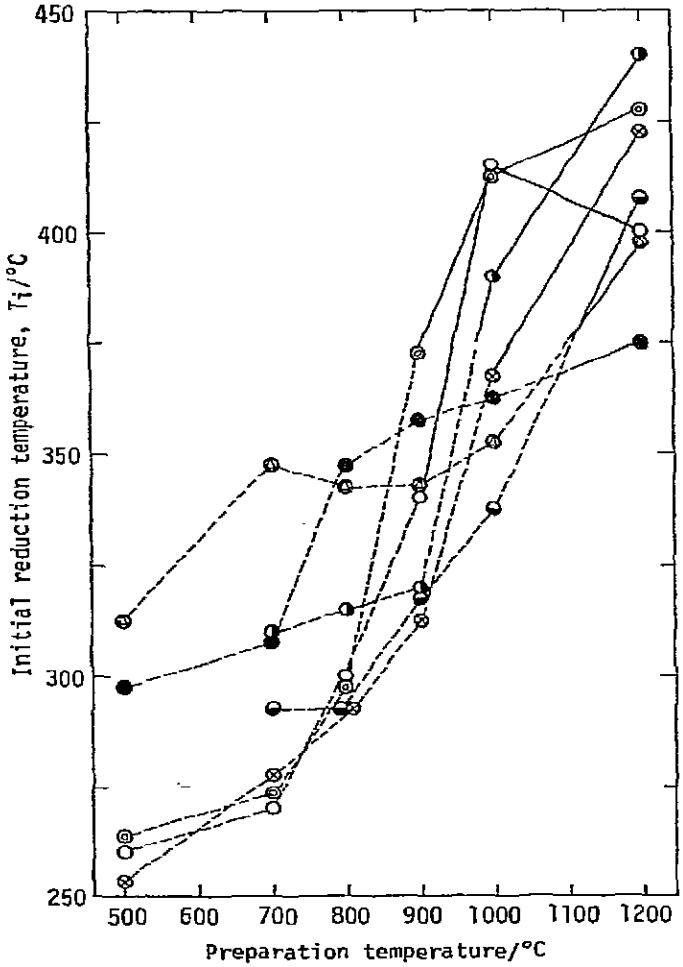

Fig. 3. Relation between the initial reduction temperature (T_i) and the preparation temperature of α-Fe_2O_3. ○, α-Fe_2O_3(A); ◑, α-Fe_2O_3(S_1); ◒, α-Fe_2O_3(S_2); ●, α-Fe_2O_3(O); ⊗, α-Fe_2O_3(N); ⊘, α-Fe_2O_3(C); ◎, α-Fe_2O_3(H). – – – –, Group(I); ——, group(II).

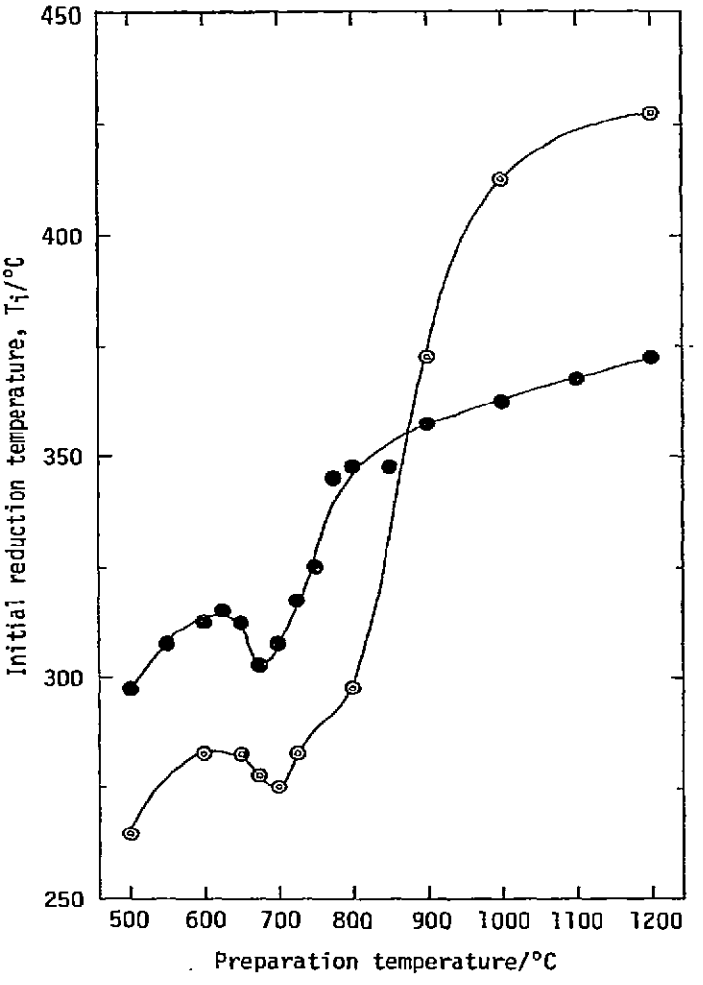

Fig. 4. Detailed relation between the initial reduction temperature (T_i) and the preparation temperature of α-Fe_2O_3 prepared in the temperature range 600–800°C. ●, α-Fe_2O_3(O); ◎, α-Fe_2O_3(H).

rather stable to hydrogen[7], was detected by X-ray diffraction of samples heated up to 600°C. The decrease in reduction rate at above 600°C may be due to FeO, which is stable above 570°C.

Figure 2 shows the TG curves of the hydrogen reduction of α-$Fe_2O_3(S_1)$ prepared in air. Curves (a)–(e) correspond to those for α-$Fe_2O_3(S_1)$ prepared at 700, 800, 900, 1000 and 1200°C, respectively. The T_i increases from 310 to 440°C with an increase in the preparation temperature between 700 and 1200°C. In a similar manner to that in the case of α-Fe_2O_3(A), Fig. 1(A), α-$Fe_2O_3(S_1)$ can be divided into two groups.

Figure 3 shows the relation between the preparation temperature of seven α-Fe_2O_3 and the measured T_i. It is found that α-Fe_2O_3 prepared at the lowest decomposition temperature from each iron salt gives the lowest T_i value, i.e. the highest reactivity for the hydrogen reduction. The value of T_i increases with increasing oxide preparation temperature, whereas T_i appears to increase much more steeply above

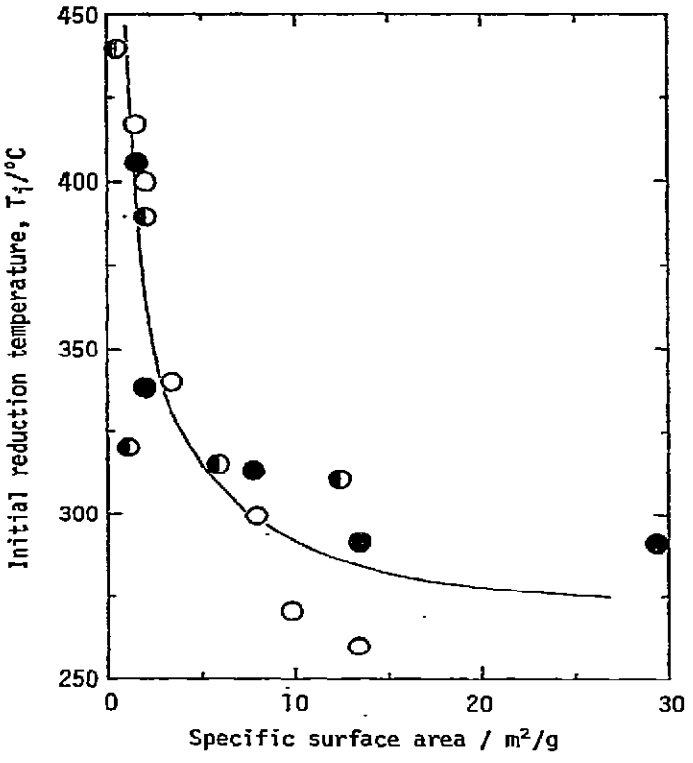

Fig. 5. Relation between initial reduction temperature (T_i) and specific surface area of α-Fe_2O_3. ○, α-Fe_2O_3(A); ◐, α-Fe_2O_3(S_1); ●, α-Fe_2O_3(S_2).

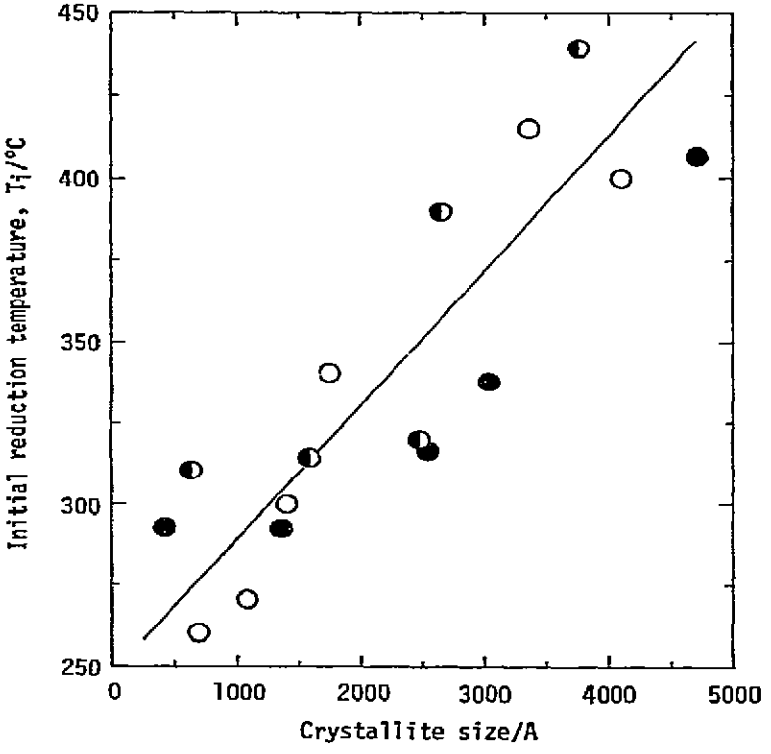

Fig. 6. Relation between the initial reduction temperature (T_i) and the crystallite size of α-Fe_2O_3. ○, α-Fe_2O_3(A); ◐, α-Fe_2O_3(S_1); ●, α-Fe_2O_3(S_2).

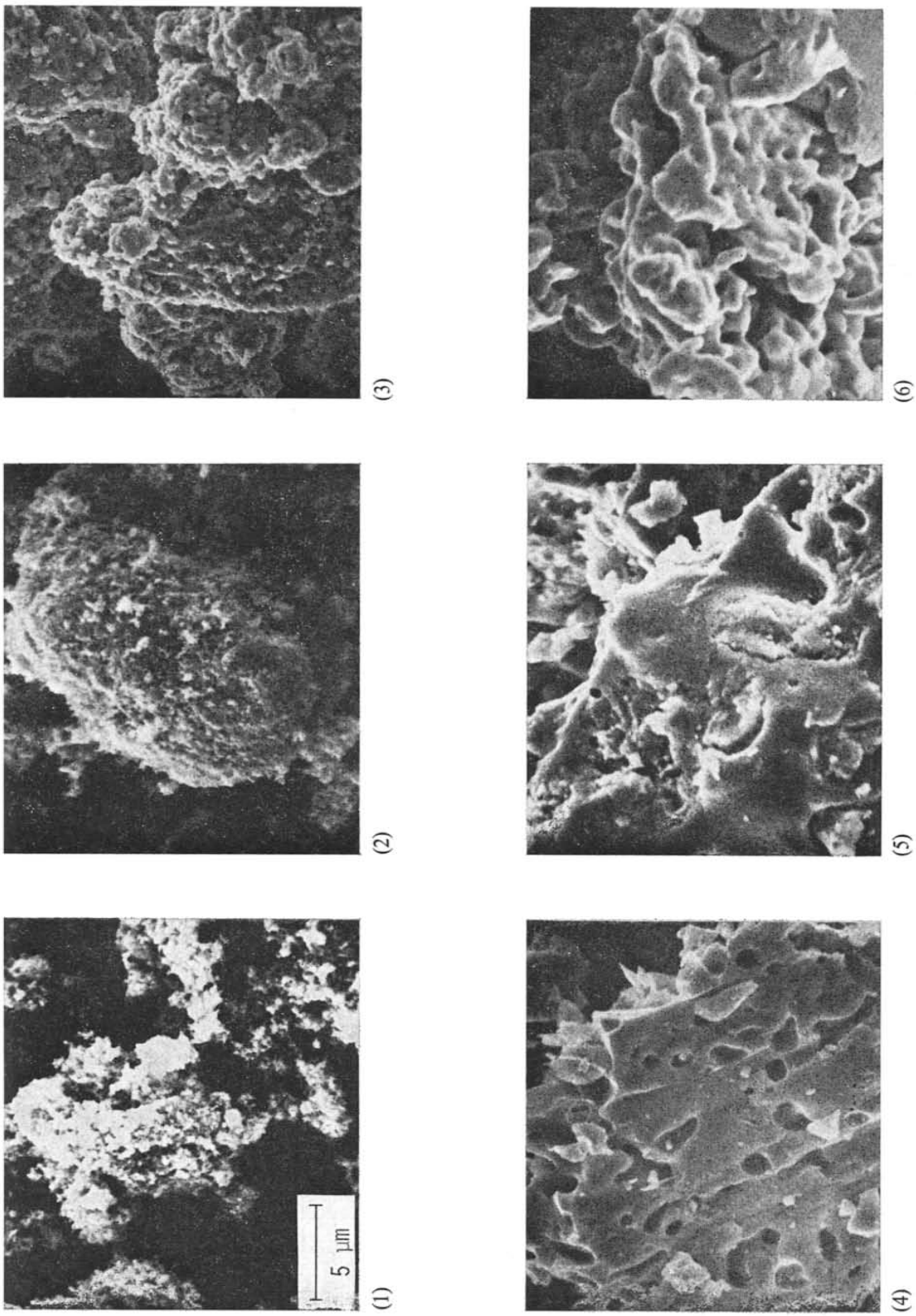

Fig. 7. SEM photographs of TG samples obtained at different stages of reduction. (1)–(3), α-Fe_2O_3 (A-500). (1), α-Fe_2O_3 (unreacted sample); (2), at 372°C (Fe_3O_4); (3), at 800°C (α-Fe). (4)–(6), α-Fe_2O_3(A-1200). (4), α-Fe_2O_3 (unreacted sample); (5), at 474°C (α-Fe_2O_3, Fe_3O_4, α-Fe); (6), at 800°C (α-Fe).

700 °C. Any clear dependence of T_i on the kind of iron salt used as starting material is not observed between 500 and 1200 °C, which may indicate that the properties of the oxide for the hydrogen reduction were little affected by the anion of iron salts. As shown in Fig. 3, the reduction of group (I) (dotted lines) proceeds in the oxide with T_i below 375 °C. As the preparation temperature of 700 °C seems to be a characteristic one, many T_i values were measured in the temperature range 600–800 °C for two samples [α-Fe_2O_3(O) and (H)]. The results are shown in Fig. 4. A marked decrease in T_i can be observed at temperatures near 700 °C. A similar change has been reported[2] in the catalytic decomposition of $KClO_4$. It may be interpreted that these phenomena are due to the Hedvall effect since the Curie and Tammann temperatures are near 700 °C.

Figure 5 shows the decreasing tendency of T_i against an increase in the specific surface area of α-Fe_2O_3(A), (S_1), and (S_2). Figure 6 shows the relation between T_i and the crystallite size of three kinds of α-Fe_2O_3. T_i seems to increase almost linearly with an increase in the crystallite size.

Figure 7 presents typical SEM photographs showing the reduction process of α-Fe_2O_3(A-500) and (A-1200). The photographs (1)–(6) correspond to the samples shown by the arrows on DTG curves in Fig. 1(B), respectively. The results of X-ray analysis are shown in parentheses. Photographs (1), (2) and (3) correspond to the unreacted α-Fe_2O_3(A-500) and the samples taken at 372 °C (11.1 % reduction) and 800 °C (completely reduced). Photographs (4), (5) and (6) correspond to the unreacted α-Fe_2O_3(A-1200), the samples taken at 474 °C (11.1 % reduction) and 800 °C. In the case of α-Fe_2O_3(A-500), the unreacted sample (1) shows an aggregation of very fine

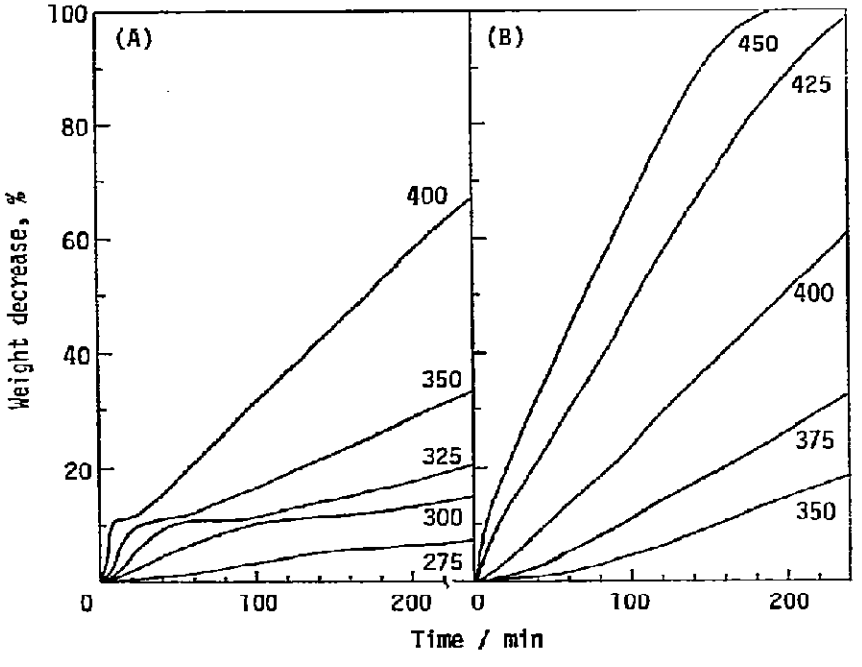

Fig. 8. Fractional reduction vs. time curves of α-Fe_2O_3(A). (A) α-Fe_2O_3(A-500); (B) α-Fe_2O_3 (A-1200).

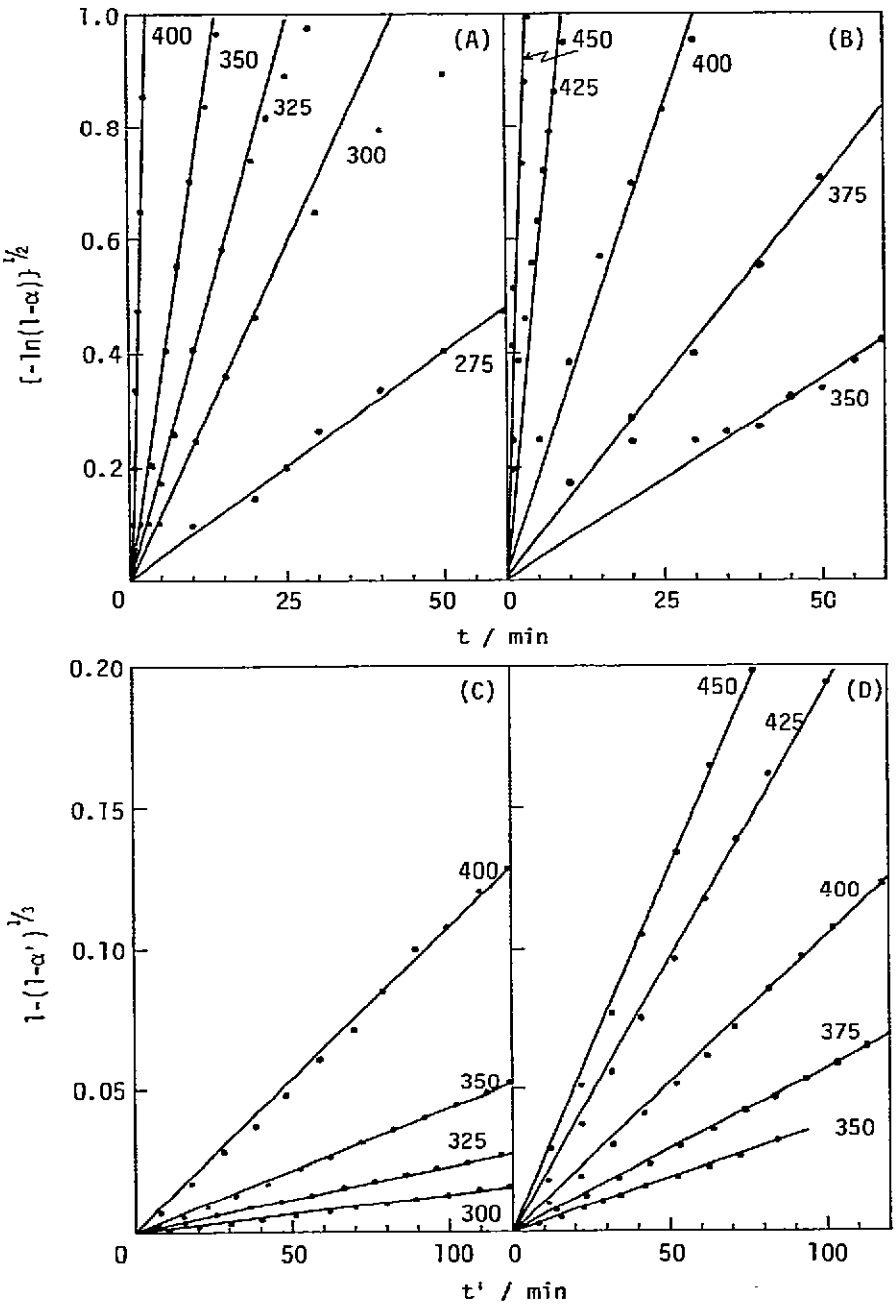

Fig. 9. Plots of $\{-\ln(1-\alpha)\}^{1/2}$ and $1-(1-\alpha')^{1/3}$ against time for the results in Fig. 8. (A) α-Fe_2O_3(A-500) (1st step reduction); (B) α-Fe_2O_3(A-1200) (1st step reduction); (C) α-Fe_2O_3(A-500) (2nd step reduction); (D) α-Fe_2O_3(A-1200) (2nd step reduction).

particles. The 11.1% reduced sample (2), which was identified as pure Fe_3O_4 by X-ray analysis, shows no change in the shape compared with that of the unreacted sample (1). The completely reduced sample (3) has a lustrous surface and it shows a compact aggregation of very fine particles. On the other hand, in the case of α-Fe_2O_3 (A-1200), the unreacted sample (4) shows a large particle with flat surface which

suggests melting of the oxide. The 11.1% reduced sample (5), which consists of α-Fe_2O_3, Fe_3O_4 and α-Fe, shows a surface characterized by cracks and shape different from that of unreacted sample (4). The sample (6) reduced at up to 800°C has a similar form to that of the completely reduced sample (3) of α-Fe_2O_3(A-500), but each particle is larger than that of (3). It may be considered that α-Fe_2O_3(A-500) with a high reactivity consists of small particles and is one reduced while keeping its particle shape unchanged, in contrast to that α-Fe_2O_3(A-1200) with a low reactivity which consists of large flat shape particles and reduced with changes in its particle shape and size.

Figures 8(A) and (B) show the weight decrease of α-Fe_2O_3(A-500) and (A-1200) as a function of time at various temperatures. In the case of α-Fe_2O_3(A-500), all curves show the plateau at 11.1% in a similar manner to TG curve in Fig. 1(A). The reduction process of the oxide can be divided into two steps as shown in eqns. (1) and (2). The weight decreases below 11.1% correspond to the reduction of α-Fe_2O_3 to Fe_3O_4, eqn. (1). The rate in the initial periods can be expressed by eqn. (3), Avrami–Erofeev's equation[14, 15] on the basis of the random nucleation mechanism, as shown in Fig. 9(A).

$$\{-\ln(1-\alpha)\}^{1/2} = kt \tag{3}$$

The value of α in eqn. (3) was normalized in such a way that the measured weight decrease of $0 \sim 11.1\%$ is equal to $\alpha = 0 \sim 1$. The activation energy of 17.7 kcal $mole^{-1}$ was estimated from the data in Fig. 9(A). On the other hand, the weight decrease above 11.1%, which correspond to the reduction of Fe_3O_4 to the metallic iron [eqn. (2)], can be expressed by Mampel's equation[16] on the basis of the phase boundary controlled reaction mechanism [eqn. (4)] as shown in Fig. 9(C). The activation energy of 14.3 kcal $mole^{-1}$ was estimated

$$1-(1-\alpha')^{1/3} = k't' \tag{4}$$

The value of α' in eqn. (4) was calculated by normalizing measured weight decrease of $11.1 \sim 100\%$ to $\alpha' = 0 \sim 1$ and time t' was calculated by taking the time at 11.1% as $t' = 0$. The similar kinetic plots for α-Fe_2O_3(A-1200) are shown in Fig. 9(B) and (D). The activation energies of 28.1 and 17.4 kcal $mole^{-1}$ were estimated from these data, respectively.

From these results, it is found that, in the reduction below 11.1%, the rate constant k of α-Fe_2O_3(A-500) is larger than that of α-Fe_2O_3(A-1200) by a factor of 6–8 and the activation energy for the oxide prepared at lower temperature is lower by about 10 kcal $mole^{-1}$ than that for the oxide prepared at higher temperature. On the other hand, in the reduction above 11.1%, both oxides exhibit similar k' values and the activation energy. Consequently, it is found that the reactivity of α-Fe_2O_3 depends on the preparation temperature, but the reactivity of Fe_3O_4 formed is almost independent of the difference in the preparation temperature of α-Fe_2O_3.

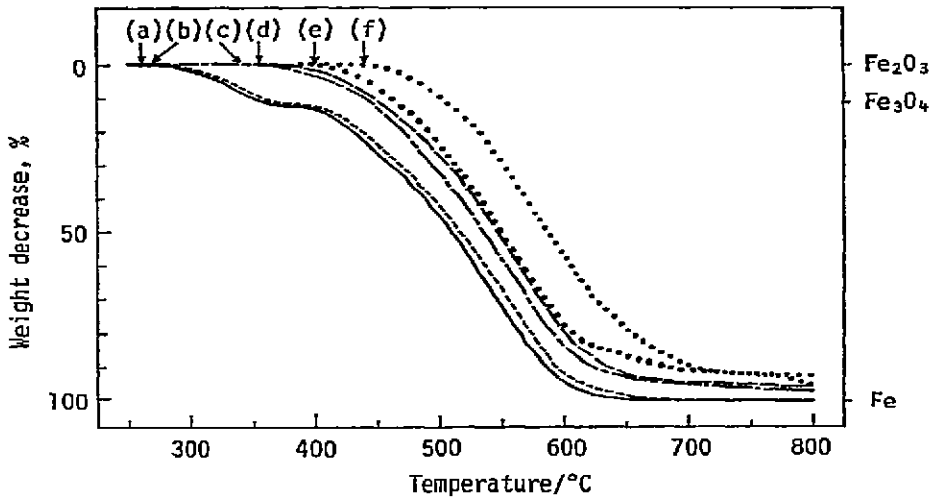

Fig. 10. TG curves of hydrogen reduction of α-Fe_2O_3(A) prepared in air and oxygen. (a) ——, α-Fe_2O_3(A-500) in air; (b) --------, α-Fe_2O_3(A-500) in oxygen; (c) — — —, α-Fe_2O_3(A-900) in air; (d) ———, α-Fe_2O_3(A-900) in oxygen; (e) ○○○○○○○, α-Fe_2O_3(A-1200) in air; (f) ....., α-Fe_2O_3 (A-1200) in oxygen. ↓ = Initial reduction temperature (T_i).

TABLE 2

INITIAL REDUCTION TEMPERATURE (T_i) OF α-Fe_2O_3 PREPARED IN VARIOUS ATMOSPHERES

α-Fe_2O_3 sample	*Preparation atmosphere*	*Preparation temperature (°C)*					
		500	*700*	*800*	*900*	*1000*	*1200*
α-Fe_2O_3(A)	Oxygen	270	275	320	355	440	440
	Air	260	270	300	340	415	400
α-Fe_2O_3(O)	Oxygen	310	340	350	360		385
	Air	295	300	345	355	360	370
α-Fe_2O_3(H)	Oxygen	265	285	300	390	425	430
	Air	265	270	295	370	410	425
	Nitrogen	260	280	290	370	390	400

TABLE 3

CHANGE IN SPECIFIC SURFACE AREA (S) AND CRYSTALLITE SIZE (d) OF α-Fe_2O_3(A)

		Preparation temperature (°C)							
		500	*600*	*700*	*800*	*900*	*1000*	*1100*	*1200*
α-Fe_2O_3	S(m^2/g)	13.5	11.6	9.9	8.0	3.5	1.5	1.9	2.0
(in air)	d(Å)	710	880	1110	1420	1750	3360	3950	4110
α-Fe_2O_3	S(m^2/g)	15.8	13.1	10.3	6.7	4.8	1.9	1.7	0.6
(in oxygen)	d(Å)	730	850	1000	1600	2100	3010	2910	3770

Influence of preparation atmosphere

Figure 10 shows the typical TG curves of α-Fe_2O_3(A) prepared in a stream of air or oxygen. Curves (a), (c) and (e) correspond to samples prepared in a stream of air at 500, 900 and 1200°C, and curves (b), (d) and (f) correspond to samples prepared in a stream of oxygen at 500, 900 and 1200°C, respectively. The arrows on the TG curves indicate T_i. T_i values of α-Fe_2O_3 prepared in oxygen are higher than in air. Table 2 shows T_i values of α-Fe_2O_3(A), (O) and (H) prepared in oxygen, air and nitrogen. It is found that the oxygen atmosphere results in higher T_i values than the air over the whole preparation temperature range. α-Fe_2O_3(H) prepared in nitrogen shows similar T_i values to those in air at preparation temperatures below 900°C, but they become lower than those in air at 1000°C and 1200°C. In general, it is found that higher oxygen partial pressure in the preparation atmosphere leads to higher T_i values. Table 3 shows specific surface area and crystallite size of α-Fe_2O_3(A) prepared in air and oxygen at 500–1200°C. The increase in the preparation temperature results in a decrease of the surface area and an increase in the crystallite size, but these values are little affected by the preparation atmospheres. Therefore, the effect of preparation atmosphere on T_i is not explicable from the difference in the surface area and the crystallite size.

Influence of doping by metal ions

Figure 11 shows TG curves of α-Fe_2O_3(S_1D) containing Ni^{2+} and Cu^{2+} ions. The T_i of undoped oxide (a) is 310°C, while the T_i of doped oxides with Ni^{2+} and Cu^{2+} ions (b and c) are 260°C and 210°C, respectively. The complete reduction temperature reached is also lowered by the doping of these ions. Table 4 shows T_i, the specific surface area and the crystallite size for α-Fe_2O_3(S_1D) containing 1 mole % of nine metal ions, and the ionic radius[17] of doping ions. It is found that the

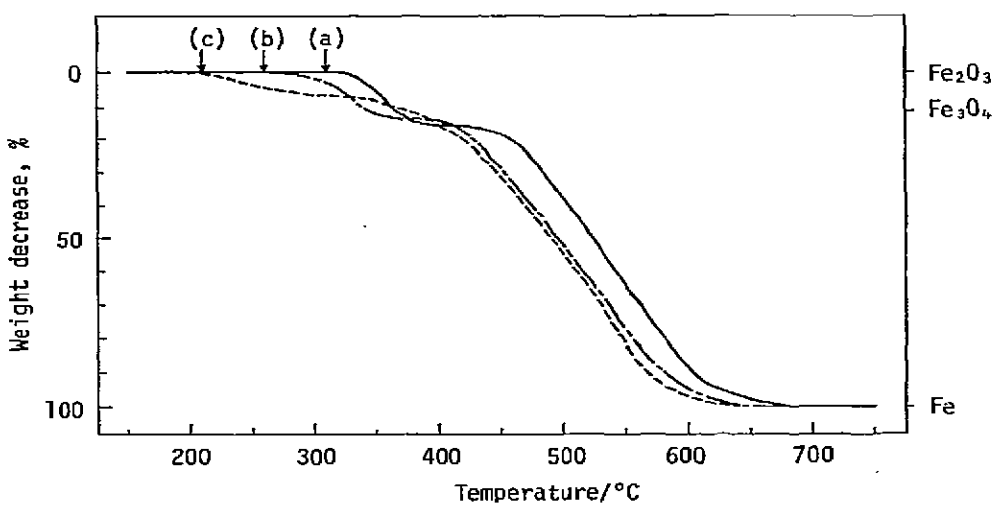

Fig. 11. TG curves of the hydrogen reduction of α-Fe_2O_3(S_1D). (a) ——, α-Fe_2O_3(S_1-700); (b) —·—, α-Fe_2O_3(S_1D-700.Ni^{2+}); (c) – – – –, α-Fe_2O_3(S_1D-700.Cu^{2+}). ↓ = Initial reduction temperature (T_i).

TABLE 4

EFFECT OF VARIOUS METAL IONS ON THE INITIAL REDUCTION TEMPERATURE (T_i), SPECIFIC SURFACE AREA (S) AND CRYSTALLITE SIZE (d) OF α-Fe_2O_3(S_1D)

M^{n+} (1 mole %)	T_i (°C)	S (m^2/g)	d (Å)	Ionic radius[17] (Å)
Fe^{3+} (pure)	310	10.7	800	0.69
Li^{+}	295	13.0	2580	0.88
Si^{4+}	285	17.1	1110	0.54
Al^{3+}	280	15.8	1330	0.67
Mg^{2+}	275		1000	0.86
Cr^{3+}	275	16.3	1010	0.76
Mn^{2+}	270		1560	0.81
Co^{2+}	270	17.3	820	0.79
Ni^{2+}	260	15.2	1330	0.84
Cu^{2+}	210	7.4	> 5000	0.87

TABLE 5

EFFECT OF VARIOUS METAL IONS ON THE INITIAL REDUCTION TEMPERATURE (T_i) AND CRYSTALLITE SIZE (d) OF α-Fe_2O_3(MD)

M^{n+} (1 mole %)	T_i (°C)	d (Å)	Ionic radius[17] (Å)
Fe^{3+} (pure)	320	960	0.69
Li^{+}	320	920	0.88
Ti^{3+}	300	900	0.81
B^{3+}	280	630	0.26
Cu^{2+}	200	760	0.87

doping of metal ion leads to a lowering of T_i by 15–100 °C, and divalent transition metal ions have a remarkable effect on the lowering of T_i. The specific surface area of the doped oxides are generally larger than that of the pure oxide, but Cu^{2+} ion shows a smaller value than that of the pure oxide. The crystallite size and the ionic radius seem to have little correlation with T_i. Therefore, the effect of doping may be an interaction of the ion with α-Fe_2O_3. When the concentration of doping agent is increased from 1 to 50 mole %, the formation of ferrite of copper and nickel, and solid solution of manganese and chromium were identified by X-ray analysis.

Table 5 shows T_i and the crystallite size of α-Fe_2O_3(MD) prepared at 600 °C by the oxidation of Fe_3O_4 doped with 1 mole % of doping agents. Cu^{2+} ion shows the lowest T_i value. The same fact is also observed for α-Fe_2O_3(S_1D) in Table 4.

Figure 12 shows the relation between the preparation temperature of α-Fe_2O_3

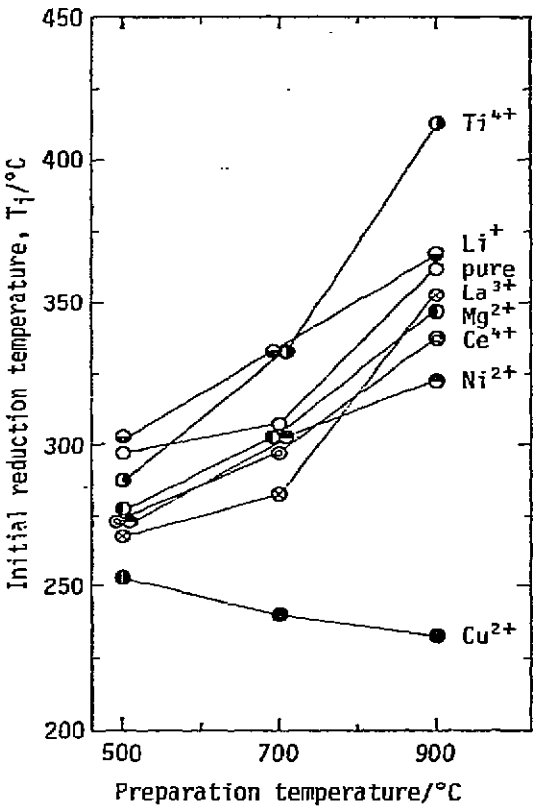

Fig. 12. Relation between the initial reduction temperature (T_i) and the preparation temperature of α-Fe_2O_3(OD) containing various metal ions.

(OD) containing a metal ion and T_i. T_i values of α-Fe_2O_3(OD) doped with the transition metal ions (Cu^{2+}, Ni^{2+}) and the lanthanoid metal ions (La^{3+}, Ce^{4+}) are lower than that of pure oxide. The doping of Li^+ and Ti^{4+} ions, however, results in higher T_i values. All T_i values except for Cu^{2+} ion increase with an increase in the preparation temperature. Cu^{2+} ion leads to a slight decrease in T_i.

DISCUSSION

Influence of preparation temperature

The reduction process of ferric ion for the initial stage is considered to be

$$O^{2-}_{(surface)} + H_{2(adsorbed)} \rightarrow H_2O_{(gas)} + 2\,e^- \quad (5)$$

$$2\,Fe^{3+}_{(surface)} + 2\,e^- \rightarrow 2\,Fe^{2+}_{(surface)} \quad (6)$$

The reason for the increase in T_i with the preparation temperature is considered to be as follows. Equations (5) and (6) suggest that T_i depends on the hydrogen adsorption power and the activity of the oxide ion. The activity of the oxide ion will be higher in disorderly oxide than in orderly oxide. The crystallite size of the oxide is increased and the surface area is decreased with an increase in the preparation tempera-

ture. It is considered, therefore, that α-Fe_2O_3 prepared at lower temperature is more disorderly and highly defective than the oxide of higher temperature preparation. Accordingly, the lower preparation temperature may result in the lower T_i.

In the reduction of oxides (group I) prepared at lower temperatures, only Fe_3O_4 was observed in the sample reduced by up to 11.1%, whereas in the reduction of oxides (group II) prepared at higher temperatures, Fe, Fe_3O_4 and α-Fe_2O_3 were observed in the sample. Whether the reduction type is group (I) or (II) may depend on the rate of eqns. (1) and (2) (r_1 and r_2), if α-Fe_2O_3 is not directly reduced to Fe. If (a) $r_1 \gg r_2$, Fe_3O_4 will accumulate, (b) $r_1 \ll r_2$, Fe_3O_4 formed will be rapidly consumed to give Fe, and (c) $r_1 \simeq r_2$, Fe_3O_4 and Fe will exist in a comparable amount each other. These three cases may lead to an 11.1% reduction, (a) $[Fe_3O_4] \gg [Fe], [\alpha\text{-}Fe_2O_3]$, (b) $[Fe_3O_4] \ll [Fe], [\alpha\text{-}Fe_2O_3]$, and (c) $[Fe_3O_4] \simeq [Fe] \simeq [\alpha\text{-}Fe_2O_3]$, respectively, where the brackets indicate the amount of species. It is found from Fig. 1(C) (i) and (ii) that cases (a) and (c) correspond to the oxides prepared at lower temperatures and at higher temperatures, respectively. The values of r_1 and r_2 would depend on the reactivity of α-Fe_2O_3 and Fe_3O_4, respectively. It is assumed from Figs. 8 and 9 that r_1 and r_2 is expressed by eqns. (3) and (4), respectively. Since Fig. 9(C) and (D) show that the slopes of the lines are almost the same at the same temperature, r_2 is little affected by the preparation temperature of the oxides. On the other hand, α-Fe_2O_3 prepared at lower temperatures consisting of small particles has higher reactivity, and thus a larger r_1 value, than that of the oxide prepared at higher temperature consisting of large flat particles. Accordingly, the condition of $r_1 \gg r_2$ will be realized for the low temperature oxide and $r_1 \simeq r_2$ will be realized for the high temperature oxide.

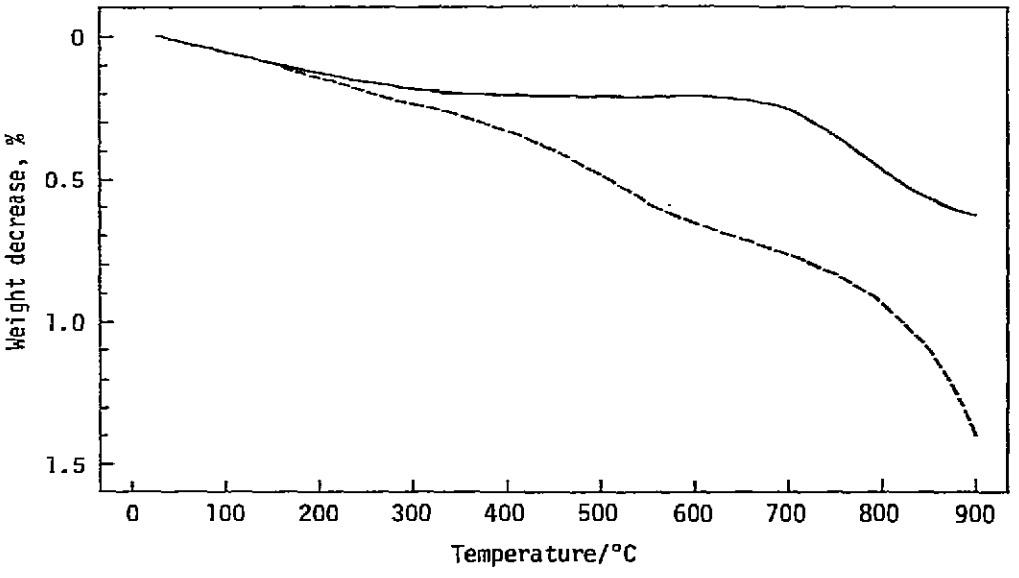

Fig. 13. TG curves of α-Fe_2O_3(O-450) in oxygen and nitrogen atmospheres. ——, In oxygen; – – – –, in nitrogen.

Influence of preparation atmosphere

It was found from Fig. 10 and Table 2 that the T_i values of α-Fe_2O_3 prepared in oxygen are higher than those of the oxides prepared in air or nitrogen; a higher oxygen partial pressure leads to lower reactivity. Figure 13 shows the TG curves of α-Fe_2O_3 in 150 mm Hg of oxygen and nitrogen in the temperature range between room temperature and 900 °C. The oxide used was α-Fe_2O_3(O-450) prepared in a stream of oxygen. The notable weight decrease, which is caused by the evolution of oxygen from the oxide, is observed at temperatures above 300 °C in nitrogen and above 650 °C in oxygen. The weight decrease observed in a nitrogen atmosphere is greater than in oxygen, and the formation of Fe_3O_4 was confirmed by X-ray analysis of the sample heated to 900 °C. α-Fe_2O_3 is usually regarded as a nonstoichiometric oxide with an oxygen deficit. It is thought that the difference in the oxygen partial pressure in the preparation atmosphere results in the difference in the activity of oxide ion and in the concentration of oxygen defect. Consequently, α-Fe_2O_3 prepared in air or nitrogen will be much more defective and thus more reducible than the oxide prepared in oxygen.

Influence of doping by metal ions

It was found from Figs. 11 and 12 and Tables 4 and 5 that the doping of metal ions except Ti^{4+} gives a rise to a higher reactivity of α-Fe_2O_3; the Cu^{2+} ion, especially, shows the most remarkable effect. The difference in T_i values caused by doping was not correlated with the surface area, the crystallite size of the oxide and the ionic radii of doping ions. As mentioned above, the reduction rate of α-Fe_2O_3 to Fe_3O_4, eqn. (1), is controlled by the nucleation process. Accordingly, the lowering of T_i caused by the doping is presumed to be due to an increase in the ability for the nucleation on the oxide surface. T_i values of the oxides of doping metals shown in Table 4, which were measured under the same experimental conditions as in α-Fe_2O_3, are 180 °C(CuO), 200 °C(MnO_2), 235 °C(Co_3O_4), 255 °C(NiO) and 275 °C (α-Fe_2O_3; commercial). Other oxides were not reduced at temperatures up to 800 °C. This fact may show that the reducible oxides lead to a lowering of the T_i of α-Fe_2O_3. As already mentioned, a small amount of ferrites or solid solutions can be formed on the surface of α-Fe_2O_3 by doping of the transition metal ions. It may be presumed that the activity of the oxide ion of α-Fe_2O_3 and the hydrogen adsorption power of the oxide will be increased by the formation of ferrite, solid solution or these embryo. In fact, the initial reduction temperature of copper and nickel ferrites were observed to be lower than that of α-Fe_2O_3 prepared at the same temperature as in ferrites. Accordingly, the nucleation on the oxide surface will depend on the surface concentration of reducible oxide ion. The reduction of α-Fe_2O_3 to Fe_3O_4 was observed to be appreciably enhanced by the presence of CuO even when the oxide was merely mixed mechanically without calcination. It can be considered[5] that this effect is provided by the hydrogen adsorbed on copper metal which was produced by the reduction of CuO, whereas Cr_2O_3, Al_2O_3, La_2O_3, MgO, SiO_2, TiO_2, etc. were not reduced under the same conditions at up to 800 °C. These oxides, however, also lead to a lowering of the T_i of

α-Fe_2O_3. Cr_2O_3 was found to form a solid solution with α-Fe_2O_3 and other oxides may form a solid solution or ferrite.

On the other hand, doping with Ti^{4+} ion at higher preparation temperature resulted in an increase in T_i of α-Fe_2O_3(OD), Fig. 12. The formation of Fe_2TiO_5 was identified by X-ray analysis in the equimolar mixture of α-Fe_2O_3 and TiO_2 calcined above 900 °C. It was observed that Fe_2TiO_5 is more difficult to reduce than α-Fe_2O_3; the initial reduction temperature of Fe_2TiO_5 prepared by calcination of α-Fe_2O_3(O) and TiO_2 at 1200 °C was 490 °C, whereas that of α-Fe_2O_3(O-1200) was 385 °C. Accordingly, the decrease in the reactivity by doping of Ti^{4+} ion will be interpreted as being due to a coating effect of Fe_2TiO_5 layer on the surface of α-Fe_2O_3(OD).

REFERENCES

1 M. Shimokawabe, R. Furuichi and T. Ishii, *Thermochim. Acta*, 21 (1977) 273.
2 M. Shimokawabe, R. Furuichi and T. Ishii, *Thermochim. Acta*, 24 (1978) 69.
3 R. Furuichi, M. Shimokawabe and T. Ishii, *Proc. Fifth Int. Conf. Therm. Anal.*, 1977, p. 512.
4 U. Colombo, F. Gazzarrini and G. Lanzavecchia, *Mater. Sci. Eng.*, 2 (1967) 125.
5 Y. Murata and N. Kasaoka, *J. Chem. Soc. Jpn., Ind. Chem. Sect.*, 61 (1958) 1440; 62 (1959) 1189; 62 (1959) 1195; 63 (1960) 1190.
6 M. Yano, A. Moriyama and T. Imoto, *J. Chem. Soc. Jpn., Ind. Chem. Sect.*, 65 (1962) 485; 66 (1963) 1289; 66 (1963) 1407.
7 W. M. Mckewan, *Trans. Metall. Soc. AIME*, 218 (1960) 2; 221 (1961) 140; 224 (1962) 2.
8 E. Kawasaki, J. Sanscrainte and T. J. Walsh, *AIChEJ*, 8 (1962) 48.
9 N. A. Warner, *Trans. Metall. Soc. AIME*, 230 (1964) 163.
10 J. O. Edström and G. Bitsianes, *Trans. AIME*, 203 (1955) 760.
11 G. Naeser and W. Scholz, *Kolloid Z.*, B156 (1958) 1.
12 S. E. Khalafalla and P. L. Weston, Jr., *Trans. Metall. Soc. AIME*, 239 (1967) 1494.
13 W. Morawietz and H. D. Schaefer, *Arch. Eisenhuettenwes.*, 40 (1969) 523; 40 (1969) 531.
14 M. Avrami, *J. Chem. Phys.*, 7 (1939) 1103; 8 (1940) 212; 9 (1941) 177.
15 B. V. Erofeev, *Compt. Rend. Acad. Sci. URSS*, 52 (1946) 511.
16 K. L. Mampel, *Z. Phys. Chem. Abt. A*, 187 (1940) 43; 187 (1940) 235.
17 R. D. Shannon and C. T. Prewitt, *Acta Crystallogr. Sect. B*, 25 (1969) 925; 26 (1970) 1046.